SPACE-TIME CODED SOQPSK IN THE PRESENCE OF DIFFERENTIAL DELAYS

Tom Nelson
Telemetry Laboratory
424 Clyde Building
Brigham Young University
Provo, UT 84602

Michael Rice
Faculty Advisor

ABSTRACT

This paper presents a method of detecting the Tier I modulation SOQPSK when it is used in a space-time coded (STC) system in which there is a non-negligible differential delay between the received signals. Space-time codes are useful to eliminate data dropouts which occur on aeronautical telemetry channels in which transmit diversity is employed. The proposed detection algorithm employs a trellis to detect the data while accounting for the offset between the in-phase and quadrature-phase components of the signals as well as the differential delay. The performance of the system is simulated and presented and it is shown that the STC eliminates the BER floor which results from the data dropouts.

KEY WORDS

Space-Time Coding, Delay Differential, SOQPSK, Aeronautical Telemetry

INTRODUCTION

In aeronautical telemtry channels, aircraft are commonly equipped with two transmit antennas to alleviate signal outages due to aircraft shadowing. However, this configuration causes severe signal level variations at the receiver when both antennas are in view. In [1], Crummet, et al. proposed using space time coding as a solution to this problem. Their solution involves employing the Alamouti 2x1 space-time code (STC) described in [2] to overcome the interference due to the two transmit antennas.

In order to use the solution proposed in [1] it is necessary to overcome two difficulties. First, due to aircraft antenna spacing the transmitted signals may not arrive at the receiver aligned in time. The standard detection algorithm for the Alamouti STC assumes that the signals are time aligned. Second, the Alamouti STC was designed for non-offset modulations, but Tier I waveforms used on telemetry channels are offset modulations due to the need for a constant envelope signal in the transmitter.

Jo and Kim [3], Yi and Lee [4], and Nelson and Rice [5] examined the effect of arrival time differences on systems employing STC with non-offset modulations. In addition, the application of STC to constant envelope modulations has received some attention in the literature in recent years. Fitz and Zhang have studied the application of STC to continuous phase modulation (CPM) signals in [6] and [7]. Cavers examined the use of STC with MSK (OQPSK with a half sine pulse shape) in [8]. In these papers it was assumed that the transmitted signals arrived at the receiver synchronized in time so that any arrival time differences were negligible. This paper shows how the considerations necessary to deal with the arrival time differences and the offset modulations can be combined to develope an algorithm suitable for the detection of space-time encoded SOQPSK when the arrival time differences are not negligible. The algorithm uses a trellis along with the Viterbi algorithm to estimate the transmitted bits.

This paper proceeds as follows: A description of how Alamouti 2x1 STC applies to SOQPSK is given in the next section. Then an algorithm that decodes Alamouti 2x1 STC for SOQPSK with arrival time differences is developed. After this algorithm is presented, its performance is compared to non-encoded (single input, single output or SISO) SOQPSK in the results section and the conclusions of the paper are presented.

SPACE-TIME CODING WITH SOQPSK

An overview of the Alamouti 2x1 STC as it applies to non-offset modulation without differential delays is presented in [2]. As shown in that paper, the detection algorithm for non-offset modulation operates on pairs of detection filter (DF) outputs which are a function of pairs of data symbols. However, the offset between the in-phase and quadrature components of SOQPSK signals makes it impossible to partition the DF output samples so that pairs of data symbols are entirely contained within pairs of samples. The presence of non-negligible arrival time differences increases this effect. Hence, in order to detect SOQPSK when the Alamouti 2x1 STC is used and when arrival time differences are present it is necessary to implement a more complex detection algorithm. This section presents a signal model for the offset case and examines the applicability of the Alamouti detection algorithm to that case.

In [9] Hill decribes the SOQPSK waveform. The expression for the modulated signal $s(t)$ is

$$s(t) = \sqrt{\frac{4E}{T}} \cos\left[2\pi f_0 t + \phi(t, \bar{\alpha}) + \phi_0\right] \tag{1}$$

where

$$\phi(t, \bar{\alpha}) = \pi h \int_{-\infty}^{t} \sum_{-\infty}^{\infty} \alpha_i g\left(\tau - \frac{iT}{2}\right) d\tau. \tag{2}$$

The information-bearing phase $\phi(t, \bar{\alpha})$ is determined by the ternary sequence $\alpha_i = -1, 0, 1$, the unity-area frequency pulse $g(t)$, and the modulation index h, which is equal to $1/2$ for offset QPSK [9]. The values α_i are a function of the data symbols. The frequency pulse $g(t)$ determines the spectral occupancy of the signal and the smoothness of the transitions from symbol to symbol.

This formulation presents SOQPSK as a ternary CPM signal. It can also be represented as a linear quadrature modulation using the technique described by Laurent in [10]. When it is formulated this way it can be seen that the signal takes the form of offset QPSK with pulse shaping that is a function of the frequency pulse $g(t)$–hence the name "shaped offset QPSK". The full Laurent decomposition consists of many pulses of varying length, each of which is modulated by a different set of so-called pseudo symbols. These pseudo symbols are a function of the data bits. All of these pulses can be combined into a single pulse which is modulated by the data bits in order to simplify the detection algorithm, but this single pulse representation requires the use of data dependent pulses. This representation of SOQPSK views it as a form of a trellis coded modulation where the pulse for each symbol comes from an alphabet of possible pulses.

Using this representation, the baseband SOQPSK signal can be written as

$$s(t) = \sum_n a(n) p_{a,n}\left(t - nT_s\right) + jb(n) p_{b,n}\left(t - T_s/2 - nT_s\right) \tag{3}$$

where, as before, T_s is the symbol time, $p_{a,n}(t)$ and $p_{b,n}(t)$ are the data dependent unit-energy pulse shapes with support on the interval $-LT_s \leq t \leq LT_s$, and $a(n)$ and $b(n)$ are the even and odd indexed data bits, respectively. Applying the Alamouti STC and following the convention that blocks begin with even indices, the Alamouti encoded transmissions from antenna 0 and antenna 1 for the interval $kT_s \leq t \leq (k+1)T_s$ are

$$\begin{aligned} \text{antenna 0:} \quad & a(k) p_{a,k}\left(t - kT_s\right) \\ & + jb(k) p_{b,k}\left(t - T_s/2 - kT_s\right) \\ \text{antenna 1:} \quad & a(k+1) p_{a,k}\left(t - kT_s\right) \\ & + jb(k+1) p_{b,k}\left(t - T_s/2 - kT_s\right) \end{aligned} \tag{4}$$

and for the interval $(k+1)T_s \leq t \leq (k+2)T_s$ they are

$$\begin{array}{ll} \text{antenna 0:} & -a(k+1)p_{a,k+1}\left(t-(k+1)T_s\right) \\ & +jb(k+1)p_{b,k+1}\left(t-T_s/2-(k+1)T_s\right) \\ \text{antenna 1:} & a(k)p_{a,k+1}\left(t-(k+1)T_s\right) \\ & -jb(k)p_{b,k+1}\left(t-T_s/2-(k+1)T_s\right). \end{array} \tag{5}$$

In the absence of arrival time differences, the detector processes the composite received signal and samples the DF output at $T_s/2$-spaced intervals. In a SISO detector, the carrier phase estimator derotates the received samples so that the decisions on the in-phase and quadrature components can be based on alternate samples. In the multiple-input, multiple-output (MIMO) case, it is not possible, in general, to derotate the samples to accomplish the same decoupling of the I and Q components. This is because the phase shifts imposed by h_0 and h_1 are, in general, different. As a consequence, the real and imaginary components of the $T_s/2$-spaced DF outputs together with the properties of the space-time code must be used to estimate the transmitted symbols.

When arrival time differences are not negligible it is not possible to sample the DF output at $T_s/2$-spaced intervals which are aligned with the optimum sampling time for both of the received signals simultaneously. In this case, in order to get the maximum signal strength in the samples, the DF output can be sampled in two sets of $T_s/2$-spaced intervals, each of which is aligned with one of the received signals. When these samples are interleaved, the resulting sequence contains samples which are each aligned with the optimum sampling time of one of the received signals.

If the receiver is synchronized to the first signal that arrives, and the second signal is delayed by τ, then the DF outputs can be stacked to form a vector. A matrix expression with the vector and matrix entries representing τ- or $(T_s/2-\tau)$-spaced samples results. The expression is

$$\mathbf{x} = \mathbf{RHd} + \mathbf{v} \tag{6}$$

where the column vectors $\mathbf{x}$ and $\mathbf{d}$ are given by

$$\mathbf{x} = \begin{bmatrix} \vdots \\ x\left(kT_s\right) \\ x\left(kT_s+\tau\right) \\ x\left(\left[k+\frac{1}{2}\right]T_s\right) \\ x\left(\left[k+\frac{1}{2}\right]T_s+\tau\right) \\ x\left(\left[k+1\right]T_s\right) \\ x\left(\left[k+1\right]T_s+\tau\right) \\ x\left(\left[k+\frac{3}{2}\right]T_s\right) \\ x\left(\left[k+\frac{3}{2}\right]T_s+\tau\right) \\ \vdots \end{bmatrix} \qquad \mathbf{d} = \begin{bmatrix} \vdots \\ a(k) \\ a(k+1) \\ jb(k) \\ jb(k+1) \\ a(k+1) \\ a(k) \\ jb(k+1) \\ jb(k) \\ \vdots \end{bmatrix}$$

and are the samples of the DF output and the desired data symbols, ordered as shown. The vector $\mathbf{v}$ contains the contribution of the additive noise to the detection filter output and consists of complex Gaussian random variables with zero mean and autocorrelation matrix

$$\mathbf{M} = \mathrm{E}\left\{\mathbf{v}\mathbf{v}^{\mathrm{H}}\right\} = \frac{N_0}{2}\mathbf{R}. \tag{7}$$

The matrix $\mathbf{R}$ is the DF correlation matrix given by

$$\mathbf{R} = \begin{bmatrix} R_{p,n}\left(0\right) & R_{p,n}\left(-\tau\right) & R_{p,n}\left(-\frac{T_s}{2}\right) & \cdots \\ R_{p,n}\left(\tau\right) & R_{p,n}\left(0\right) & R_{p,n}\left(-\frac{T_s}{2}+\tau\right) & \\ R_{p,n}\left(\frac{T_s}{2}\right) & R_{p,n}\left(\frac{T_s}{2}-\tau\right) & R_{p,n}\left(0\right) & \\ \vdots & & & \ddots \end{bmatrix} \tag{8}$$

where $R_p\left(\tau\right)$ is defined by

$$R_p\left(\tau\right) = \int_{-LT_s}^{LT_s} p(t)f(t+\tau)dt \tag{9}$$

where $f(t)$ is the DF impulse response. Note that the elements of $\mathbf{R}$ are data dependent due to the dependence of the pulses $p_n(t)$ on the data as explained above. This matrix is almost a Toeplitz matrix—the main diagonal and the even indexed diagonals are constant while the odd indexed diagonals alternate between two values which differ by $T_s/2-\tau$. For a pulse shape with support on the interval $-LT_s \leq t \leq LT_s$, there will be $4L-1$ non-zero diagonals above the main diagonal and $4L-1$ non-zero diagonals below the main diagonal. The matrix $\mathbf{H}$ is a block diagonal matrix defined by

$$\mathbf{H} = \begin{bmatrix} \mathbf{H_8} & \mathbf{0} & \cdots \\ \mathbf{0} & \mathbf{H_8} & \\ \vdots & & \ddots \end{bmatrix} \tag{10}$$

where

$$\mathbf{H_8} = \begin{bmatrix} h_0 & 0 & 0 & 0 & 0 & 0 & 0 & 0 \\ 0 & h_1 & 0 & 0 & 0 & 0 & 0 & 0 \\ 0 & 0 & h_0 & 0 & 0 & 0 & 0 & 0 \\ 0 & 0 & 0 & h_1 & 0 & 0 & 0 & 0 \\ 0 & 0 & 0 & 0 & -h_0 & 0 & 0 & 0 \\ 0 & 0 & 0 & 0 & 0 & h_1 & 0 & 0 \\ 0 & 0 & 0 & 0 & 0 & 0 & h_0 & 0 \\ 0 & 0 & 0 & 0 & 0 & 0 & 0 & -h_1 \end{bmatrix}. \tag{11}$$

A maximum-likelihood (ML) solution can be envisioned if a packet of N data symbols is assumed. In this case, the column vectors $\mathbf{x}$, $\mathbf{d}$, and $\mathbf{v}$ have dimension $4N \times 1$ while the matrices $\mathbf{R}$ and $\mathbf{H}$ have dimension $4N \times 4N$. The ML estimate is

$$\hat{\mathbf{d}} = \underset{\mathbf{d}\in\mathcal{S}^N}{\operatorname{argmin}} \left\{\left(\mathbf{x}-\mathbf{RHd}\right)^{\mathrm{H}}\mathbf{M}^{-1}\left(\mathbf{x}-\mathbf{RHd}\right)\right\}. \tag{12}$$

There are two difficulties that arise when attempting to solve (12). First, $\mathbf{M}$ is not a diagonal matrix because the noise sampled at τ or $T_s/2-\tau$ will generally be correlated (due to the detection filter). Second, the matrix $\mathbf{R}$ will not, in general, be a diagonal matrix. The consequence of these two facts is that the operations on the samples in $\mathbf{x}$ cannot be decoupled as they were in the non-offset case with no arrival time differences (shown in [5]).

Some conditions can be applied to simplify the solution of (12). If the pulse shape satisfies the Nyquist no-ISI condition: $R_{p,n}(mT_s) = 0$ for all non-zero integers m then the effect on $\mathbf{R}$ is to render some of the diagonals to be zero. This reduces the number of non-zero elements in $\mathbf{R}$. However, $\mathbf{R}$ is still not a diagonal matrix due to the entries that are a function of τ as well as the diagonals containing detection filter correlations at odd multiples of $T_s/2$. If, in addition to satisfying the Nyquist no-ISI condition, the pulse shape is full response then $R_p(t) = 0$ for $|t| \geq T_s$ and the number of non-zero diagonals in $\mathbf{R}$ is further decreased. As $\mathbf{R}$ becomes closer to $\mathbf{I}$, the complexity of the solution to (12) reduces. However, the presence of the $\mathbf{M}^{-1}$ term in that equation means that the operations on the samples in $\mathbf{x}$ still cannot be decoupled.

SOQPSK DECODING ALGORITHM

One approach to this problem is to make the approximation $\mathbf{M} \approx \frac{N_0}{2}\mathbf{I}$. Then (12) becomes

$$\hat{\mathbf{d}} = \underset{\mathbf{d}\in\mathcal{S}^N}{\operatorname{argmin}} \left\{ |\mathbf{x} - \mathbf{RHd}|^2 \right\}. \tag{13}$$

Hence, ignoring the correlation on the noise leads to the least squares (LS) solution.

A solution to (13) can be found by examining the quantity to be minimized. Let

$$\boldsymbol{\Delta} = \mathbf{x} - \mathbf{RHd}. \tag{14}$$

Elements in the term $\mathbf{RHd}$ in (14) can be expanded to give the expression in (15).

$$\boldsymbol{\Delta} = \begin{bmatrix} \vdots \\ x\left(\left[k+1\right]T_s+\tau\right) \\ x\left(\left[k+\frac{3}{2}\right]T_s\right) \\ x\left(\left[k+\frac{3}{2}\right]T_s+\tau\right) \\ x\left(\left[k+2\right]T_s\right) \\ x\left(\left[k+2\right]T_s+\tau\right) \\ x\left(\left[k+\frac{5}{2}\right]T_s\right) \\ x\left(\left[k+\frac{5}{2}\right]T_s+\tau\right) \\ x\left(\left[k+3\right]T_s\right) \\ \vdots \end{bmatrix} - \begin{bmatrix} \vdots \\ h_0\left[c_1(b_0,\bar{a}_1,b_1,a_2,b_2;\tau)+jc_1(a_0,b_0,\bar{a}_1,b_1,a_2;\frac{T_s}{2}+\tau)\right]+h_1\left[c_2(b_1,a_0,\bar{b}_0)+jc_1(a_1,b_1,a_0,\bar{b}_0,a_3;\frac{T_s}{2})\right] \\ h_0\left[c_1(b_0,\bar{a}_1,b_1,a_2,b_2;\frac{T_s}{2})+jc_2(\bar{a}_1,b_1,a_2)\right]+h_1\left[c_1(b_1,a_0,\bar{b}_0,a_3,b_3;\frac{T_s}{2}-\tau)+jc_1(a_1,b_1,a_0,\bar{b}_0,a_3;T_s-\tau)\right] \\ h_0\left[c_1(b_0,\bar{a}_1,b_1,a_2,b_2;\frac{T_s}{2}+\tau)+jc_1(\bar{a}_1,b_1,a_2,b_2,\bar{a}_3;\tau)\right]+h_1\left[c_1(b_1,a_0,\bar{b}_0,a_3,b_3;\frac{T_s}{2})+jc_2(a_0,\bar{b}_0,a_3)\right] \\ h_0\left[c_2(b_1,a_2,b_2)+jc_1(\bar{a}_1,b_1,a_2,b_2,\bar{a}_3;\frac{T_s}{2})\right]+h_1\left[c_1(b_1,a_0,\bar{b}_0,a_3,b_3;T_s-\tau)+jc_1(a_0,\bar{b}_0,a_3,b_3,a_2;\frac{T_s}{2}-\tau)\right] \\ h_0\left[c_1(b_1,a_2,b_2,\bar{a}_3,b_3;\tau)+jc_1(\bar{a}_1,b_1,a_2,b_2,\bar{a}_3;\frac{T_s}{2}+\tau)\right]+h_1\left[c_2(\bar{b}_0,a_3,b_3)+jc_1(a_0,\bar{b}_0,a_3,b_3,a_2;\frac{T_s}{2})\right] \\ h_0\left[c_1(b_1,a_2,b_2,\bar{a}_3,b_3;\frac{T_s}{2})+jc_2(a_2,b_2,\bar{a}_3)\right]+h_1\left[c_1(\bar{b}_0,a_3,b_3,a_2,\bar{b}_2;\frac{T_s}{2}-\tau)+jc_1(a_0,\bar{b}_0,a_3,b_3,a_2;T_s-\tau)\right] \\ h_0\left[c_1(b_1,a_2,b_2,\bar{a}_3,b_3;\frac{T_s}{2}+\tau)+jc_1(a_2,b_2,\bar{a}_3,b_3,a_4;\tau)\right]+h_1\left[c_1(\bar{b}_0,a_3,b_3,a_2,\bar{b}_2;\frac{T_s}{2})+jc_2(a_3,b_3,a_2)\right] \\ h_0\left[c_2(b_2,\bar{a}_3,b_3)+jc_1(a_2,b_2,\bar{a}_3,b_3,a_4;\frac{T_s}{2})\right]+h_1\left[c_1(\bar{b}_0,a_3,b_3,a_2,\bar{b}_2;T_s-\tau)+jc_1(a_3,b_3,a_2,\bar{b}_2,a_5;\frac{T_s}{2}-\tau)\right] \\ \vdots \end{bmatrix} \tag{15}$$

In this equation the following shorthand notation is used: a_m represents $a(k+m)$ and $\bar{a}_0$ represents $-a(k)$. The functions $c_1(\cdot)$ and $c_2(\cdot)$ in the second term in that equation provide samples from the data dependent $R_{p,n}(t)$. The five bits in the argument of $c_1(\cdot)$ provide the index for the waveform while the time argument gives the offset of the desired sample of the waveform. The function $c_2(\cdot)$ gives the data dependent peak of $R_{p,n}(0)$. Because the same bits appear in multiple elements of $\mathbf{\Delta}$, the quantity $|\mathbf{\Delta}|^2$ can be minimized by employing a trellis and the Viterbi algorithm (VA).

The trellis is implemented by reading in the block of eight MF output samples. These samples are comprised of the four samples which are aligned with $s_0(t)$: $\{x([k+\frac{3}{2}]T_s), x([k+2]T_s), x([k+\frac{5}{2}]T_s), x([k+3]T_s)\}$ (for even k) interleaved with the four samples which are aligned with $s_1(t)$: $\{x([k+1]T_s+\tau), x([k+\frac{3}{2}]T_s+\tau), x([k+2]T_s+\tau), x([k+\frac{5}{2}]T_s+\tau)\}$ (also for even k). Then the partial path metrics are updated in the trellis for each MF output. At the end of the block the decisions $(\hat{a}(k), \hat{b}(k), \hat{a}(k+1), \hat{b}(k+1))$ are output. The novel approach of this algorithm is that the branch metrics are different, depending on the position in the block. With the elements of $\mathbf{\Delta}$ expressed as

$$\mathbf{\Delta} = \begin{bmatrix} \vdots \\ \Delta\left(k+1+\tau\right) \\ \Delta\left(k+\frac{3}{2}\right) \\ \Delta\left(k+\frac{3}{2}+\tau\right) \\ \Delta(k+2) \\ \Delta(k+2+\tau) \\ \Delta\left(k+\frac{5}{2}\right) \\ \Delta\left(k+\frac{5}{2}+\tau\right) \\ \Delta\left(k+3\right) \\ \vdots \end{bmatrix}, \tag{16}$$

the branch metrics are given by

$$\lambda_{k+1+\tau}[a_0, b_0, a_1, b_1, a_2, b_2, a_3] = \left|\Delta\left(k+1+\tau\right)\right|^2 \tag{17}$$

$$\lambda_{k+\frac{3}{2}}[a_0, b_0, a_1, b_1, a_2, b_2, a_3, b_3] = \left|\Delta\left(k+\frac{3}{2}\right)\right|^2 \tag{18}$$

$$\lambda_{k+\frac{3}{2}+\tau}[a_0, b_0, a_1, b_1, a_2, b_2, a_3, b_3] = \left|\Delta\left(k+\frac{3}{2}+\tau\right)\right|^2 \tag{19}$$

$$\lambda_{k+2}[a_0, b_0, a_1, b_1, a_2, b_2, a_3, b_3] = \left|\Delta\left(k+2\right)\right|^2 \tag{20}$$

$$\lambda_{k+2+\tau}[a_0, b_0, a_1, b_1, a_2, b_2, a_3, b_3] = \left|\Delta\left(k+2+\tau\right)\right|^2 \tag{21}$$

$$\lambda_{k+\frac{5}{2}}[a_0, b_0, b_1, a_2, b_2, a_3, b_3] = \left|\Delta\left(k+\frac{5}{2}\right)\right|^2 \tag{22}$$

$$\lambda_{k+\frac{5}{2}+\tau}[b_0, b_1, a_2, b_2, a_3, b_3, a_4] = \left|\Delta\left(k+\frac{5}{2}+\tau\right)\right|^2 \tag{23}$$

$$\lambda_{k+3}[b_0, a_2, b_2, a_3, b_3, a_4, a_5] = \left|\Delta\left(k+3\right)\right|^2. \tag{24}$$

The arguments of $\lambda_n[\cdot]$ are the bits that define the states for each stage. The number of states in the trellis is either 128 or 256, depending on the number of bits that contribute to the sample under consideration in each stage. The output bits $[\hat{a}(k), \hat{b}(k), \hat{a}(k+1), \hat{b}(k+1)]$ are those that minimize the expression

$$\begin{aligned}\Gamma \;=\;& \lambda_{k+1+\tau} + \lambda_{k+\frac{3}{2}} + \lambda_{k+\frac{3}{2}+\tau} + \lambda_{k+2} + \\ & \lambda_{k+2+\tau} + \lambda_{k+\frac{5}{2}}\lambda_{k+\frac{5}{2}+\tau} + \lambda_{k+3} + +\pi_k\end{aligned} \tag{25}$$

where π_k is the partial path metric up through the stage at time $(k+1)T_s$ and is given by

$$\pi_k = \sum_{i=0}^{2k+2} \lambda_{\frac{i}{2}} + \lambda_{\frac{i}{2}+\tau}. \tag{26}$$

The sample $x((k+3)T_s)$ is the last sample which contains a contribution from any of the bits in the block $[a(k), b(k), a(k+1), b(k+1)]$. Once this sample has been processed, a decision on that block of bits can be made. After the stage at $t = (k+3)T_s$, the state with the minimum path metric is found. That state is then traced back to the stage at $t = (k+1)T_s$. The state at that stage which leads to the minimum metric state at the later stage gives the values for the output bits.

RESULTS

The trellis described in the previous section was implemented and its performance was evaluated using Monte Carlo simulations. The detection filter used for the simulations presented here was a half sine filter. In addition, it was assumed that the timing and carrier offset as well as the complex channel gains are known, and the channel varies slowly enough that it can be approximated as being constant over several symbol times. The channel gains h_0 and h_1 satisfy

$$|h_0|^2 + |h_1|^2 = 1. \tag{27}$$

The detection filtering was performed at a sample rate of 10 samples per symbol.

Fig. 1 shows the performance obtained using the algorithm described in the previous section. As can be seen, when the differential delay is negligible, the detection algorithm provides performance comparable to the theoretical performance of OQPSK. This shows that space-time encoded

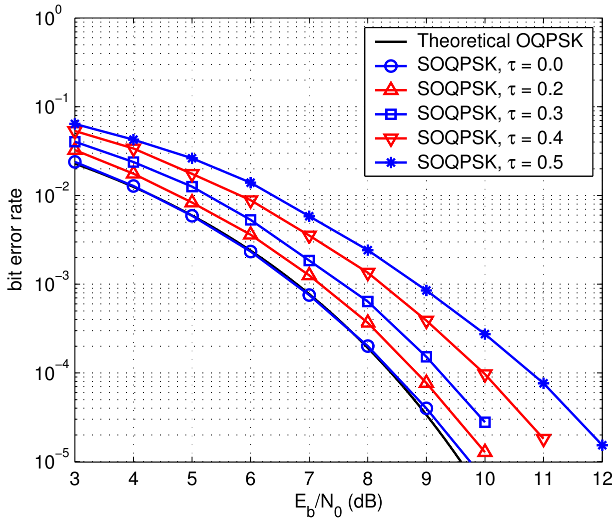

Figure 1: Bit Error rate as a function of E_b/N_0.

SOQPSK can be successfully detected. Fig. 1 also shows that the presence of a differential delay results in a degradation in detection performance. The cause of this degradation is a topic of continuing research. The absence of a floor in the BER curves for the MIMO SOQPSK detector indicates that the space-time code is successful at eliminating the data dropouts that occur when no STC is used.

CONCLUSION

An algorithm for detecting SOQPSK signals that employ the Alamouti 2x1 STC has been presented. The Viterbi algorithm is used to determine the LS estimate of the transmitted symbol sequence. The performance of this algorithm is also presented. It can be seen that this signaling method is successful in avoiding the data dropouts that can plague aeronautical telemetry channels when multiple transmit antenna are placed on the test vehicle.

REFERENCES

[1] R. C. Crummett, M. A. Jensen, and M. D. Rice, “Transmit Diversity Scheme for Dual-Antenna Aeronautical Telemetry Systems,” *Proceedings of the International Telemetry Conference*, October 2002. pp. 113–121.

[2] S. Alamouti, “A Simple Transmit Diversity Technique for Wireless Communications,” *IEEE Journal on Selected Areas in Communications*, October 1998. pp. 1451–1458.

[3] K. Jo and H. M. Kim, “Decoding of space-time codes for Rayleigh flat fading with arrival time differences,” *IEEE Electronics Letters,* vol. 36, no. 23, pp. 1936-1937, Nov. 2000.

[4] J. Yi and J. H. Lee, “Interference cancellation for a space-time coded DS-CDMA system in a rayleigh fading channel with arrival time differences,” *VTC2002*, pp. 1424-1428.

[5] T. Nelson and M. D. Rice, “Alamouti Space-time Coding for QPSK with Delay Differential,” *Proceedings of the International Telemetry Conference*, October 2003. pp. 1249-1258.

[6] M. P. Fitz and X. Zhang, “A Case for Continuous Phase Modulation in Space-Time Modems,” *ITW2002*, Bangalore, India, Oct. 20-25, 2002.

[7] X. Zhang and M. P. Fitz, “Space-Time Code Design With Continuous Phase Modulation,” *IEEE Journal on Selected Areas in Communications*, June 2003, pp. 783–792.

[8] J. K. Cavers, “Space-Time Coding Using MSK,” *Vehicular Technology Conference, 2002, Proceedings*, vol. 1, 24-28 Sept. 2002, pp. 401-405.

[9] T. Hill, “An Enhanced, Constant Envelope, Interoperable Shaped Offset QPSK (SOQPSK) Waveform for Improved Spectral Efficiency,” *Proceedings of the International Telemetry Conference*, 00-02-5, San Diego, CA, October, 2000, pp. 127-136.

[10] P. A. Laurent, “Exact and Approximate Construction of Digital Phase Modulations by Superposition of Amplitude Modulated Pulses (AMP),” *IEEE Transactions on Communications*, vol. 34, no. 2, February 1986, pp. 150-160.